

Violation of energy-per-hadron scaling in a resonance matter

L. Bravina,^{1,*} Amand Faessler,¹ C. Fuchs,¹ Zhong-Dao Lu,^{2,3} and E.E. Zabrodin^{1,*}

¹*Institut für Theoretische Physik, Universität Tübingen,
Auf der Morgenstelle 14, D-72076 Tübingen, Germany*

²*China Institute of Atomic Energy, P. O. Box 275(18), Beijing 102413, China*

³*China Center of Advance Science and Technology (CCAST), Beijing 100080, China*

(Dated: November 1, 2018)

Yields of hadrons, their average masses and energies per hadron at the stage of chemical freeze-out in (ultra)relativistic heavy-ion collisions are analyzed within the statistical model. The violation of the scaling $\langle E \rangle / \langle N \rangle \cong 1 \text{ GeV}$ observed in Au+Au collisions at $\sqrt{s} = 130A \text{ GeV}$ is linked to the formation of resonance-rich matter with a considerable fraction of baryons and antibaryons. The rise of the energy-per-hadron ratio in baryon-dominated matter is discussed. A violation of the scaling condition is predicted for a very central zone of heavy-ion collisions at energies around 40A GeV.

PACS numbers: 25.75.-q, 24.10.Pa, 25.75.Dw

The properties of nuclear matter under extreme conditions have been the subject of intensive experimental and theoretical studies during the last few decades. Up to now experiments with heavy-ion collisions remain the only means to explore the properties of hot and dense nuclear matter in the laboratory. Two energy ranges connected with predicted phase transitions in the nuclear medium have been studied especially vigorously, - the intermediate energy range, where the nuclear liquid-gas phase transition might occur, and the range of relativistic and ultra-relativistic energies, where the phase transition to a deconfined quark-gluon plasma (QGP) and a restoration of chiral symmetry should take place (see [1, 2] and references therein). The search for the QGP formation is one of the top-priority goals of the heavy-ion collider program at Relativistic Heavy Ion Collider (RHIC) in Brookhaven, which is operating since 1999, and at the forthcoming Large Hadron Collider (LHC) at CERN.

In order to reveal possible fingerprints of the QGP formation, various microscopic (transport, string, cascade) and macroscopic (thermal and hydrodynamic) models are widely used for the analysis of measured particle abundances and energy spectra. In macroscopic scenarios it is assumed that a rapidly expanding and cooling thermalized system experiences at the late stage of its evolution the so-called chemical freeze-out, where all inelastic processes have to cease, accompanied by the thermal freeze-out, which occurs when the mean free path of particles exceeds the linear sizes of the system. Therefore, the conditions of the system at the chemical freeze-out stage can be obtained from hadron abundances and ratios, which are not affected by the collective flow. The analysis of experimental data taken in a broad energy range from SIS to SPS suggests [3] that there exists a

scaling law concerning the energy per hadron ratio at the chemical freeze-out, $\langle E \rangle / \langle N \rangle \approx 1 \text{ GeV}$, while in Au+Au collisions at $\sqrt{s} = 130 \text{ AGeV}$ (RHIC) this ratio increases to $\langle E \rangle / \langle N \rangle \approx 1.1 \text{ GeV}$. Simple estimates show that in the latter case the average hadron mass should increase as well, because the chemical freeze-out temperature at RHIC does not exceed that at SPS by more than 10-20 MeV [4]. In the present paper we argue that the rise of the average hadron energy and mass at RHIC is caused by the transition to dense meson-resonance rich matter with a considerable fraction of baryons and antibaryons. Another substance with peculiar characteristics is baryon-dominated resonance matter, which can be formed in heavy-ion collisions at bombarding energies between 10 AGeV and 40 AGeV, accessible for the accelerator planned at GSI. Here the energy per hadron at chemical freeze-out increases as well.

For our study we use a conventional statistical model (SM) of an ideal hadron gas [3, 4, 5, 6, 7, 8, 9, 10, 11] which enables one to determine all macroscopic characteristics of a system at given temperature T , baryon chemical potential μ_B , and strangeness chemical potential μ_S via the set of distribution functions (in units of $c = k_B = \hbar = 1$)

$$f(p, m_i) = \left[\exp \left(\frac{E_i - \mu_i}{T} \right) \pm 1 \right]^{-1} \quad (1)$$

Here m_i , $E_i = \sqrt{p^2 + m_i^2}$, p , and μ_i are the mass, energy, momentum, and the chemical potential of hadron species i , respectively. Denoting baryon and strange charges of the i th particles as B_i and S_i one can write $\mu_i = B_i \mu_B + S_i \mu_S$. The electrochemical potential considered in [10] and the isospin chemical potential considered in [4, 5] are neglected. The sign "+(-)" in Eq. (1) corresponds to fermions (bosons). The particle number density n_i , the energy density ε_i and the partial pressure P_i read

$$n_i = \frac{g_i}{(2\pi)^3} \int_0^\infty f(p, m_i) d^3p, \quad (2)$$

*Also at Institute for Nuclear Physics, Moscow State University, RU-119899 Moscow, Russia

$$\varepsilon_i = \frac{g_i}{(2\pi)^3} \int_0^\infty \sqrt{p^2 + m_i^2} f(p, m_i) d^3p, \quad (3)$$

$$P_i = \frac{g_i}{(2\pi)^3} \int_0^\infty \frac{p^2}{3(p^2 + m_i^2)^{1/2}} f(p, m_i) d^3p, \quad (4)$$

with g_i being the spin-isospin degeneracy factor of hadron i . Instead of evaluating of the integrals in Eqs. (2)-(4) by replacing of Fermi-Dirac or Bose-Einstein distribution functions (1) to Maxwell-Boltzmann ones

$$f^{MB}(p, m_i) = \exp\left(\frac{\mu_i - E_i}{T}\right) \quad (5)$$

we employ the series expansion of (1) in a form [6]

$$f(p, m_i) = \sum_{n=1}^{\infty} (\mp 1)^{n+1} \exp\left(-n \frac{E_i - \mu_i}{T}\right), \quad (6)$$

which is inserted to Eqs. (2)-(4). After some straightforward calculations one gets

$$n_i = \frac{g_i m_i^2 T}{2\pi^2} \sum_{n=1}^{\infty} \frac{(\mp 1)^{n+1}}{n} \exp\left(\frac{n\mu_i}{T}\right) K_2\left(\frac{nm_i}{T}\right) \quad (7)$$

$$\varepsilon_i = \frac{g_i m_i^2 T^2}{2\pi^2} \sum_{n=1}^{\infty} \frac{(\mp 1)^{n+1}}{n^2} \exp\left(\frac{n\mu_i}{T}\right) \times \left[3K_2\left(\frac{nm_i}{T}\right) + \frac{nm_i}{T} K_1\left(\frac{nm_i}{T}\right) \right] \quad (8)$$

$$P_i = \frac{g_i m_i^2 T^2}{2\pi^2} \sum_{n=1}^{\infty} \frac{(\mp 1)^{n+1}}{n^2} \exp\left(\frac{n\mu_i}{T}\right) K_2\left(\frac{nm_i}{T}\right) \quad (9)$$

where K_1 and K_2 are modified Hankel function of first and second order. For $n = 1$ the results with the Maxwell-Boltzmann distribution (5) are regained [12].

The equation of state (EOS) of an ideal hadron gas in the form $\langle E(T, \mu_B) \rangle / \langle N(T, \mu_B) \rangle$ and the average hadron

mass $\langle M(T, \mu_B) \rangle = 1/N \sum_{i=1}^N m_i$ are shown in Fig. 1. The

calculations are performed within the standard SM at zero net strangeness in the system. The increase of both quantities can be caused either by the rise of the temperature of the system or by an increasing baryon chemical potential, which is directly linked to the baryon density. Both macroscopic [4] and microscopic [13] models indicate that the case with low μ_B and relatively high T is relevant for Au+Au collisions at RHIC. To study the conditions of chemical freeze-out we also apply a generalization of the SM to two thermal sources (TSM) proposed in [14], which accounts for possible inhomogeneities of the net baryon charge, observed experimentally e.g. at SPS energies (158 AGeV/c) [15], and net strangeness distribution inside the reaction volume. The idea behind the TSM is quite simple. It is well known (see, e.g., [3]) that the hadron ratios in the system consisting of several fireballs are not affected by longitudinal or transverse collective motion of sources, provided all fireballs have

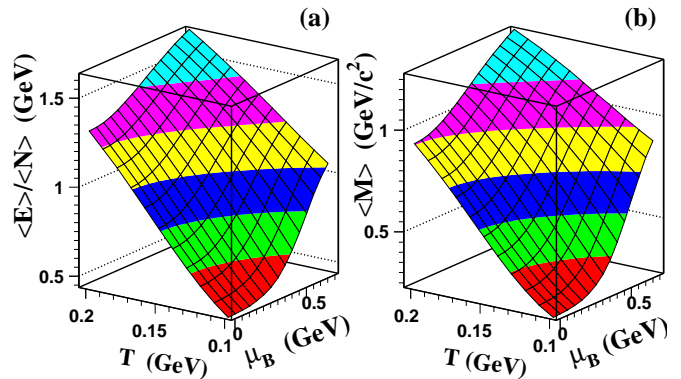


FIG. 1: (a) Average energy per hadron and (b) average hadron mass as functions of the temperature T and the baryo-chemical potential μ_B of the system.

the same baryon chemical potential and the same temperature. In this case the particle ratios are identical to those obtained for a single static source. If, for instance, the baryon charge or strangeness is not homogeneously distributed within the total volume, the problem cannot be reduced to a single source scenario. In the TSM the whole system is separated in two parts, which at SPS and lower energies can most naturally be interpreted as an inner source (or core) and an outer source (or halo), each being in local thermal and chemical equilibrium, i.e. their (local) macroscopic characteristics are determined by Eqs. (2) - (4). However, their temperatures, baryon and strangeness chemical potentials are allowed (but not postulated) to be different. No additional constraints are assumed in the model except of the total strangeness conservation $N_S^{tot} = N_S^{(1)} + N_S^{(2)} = 0$.

A fit to experimental data at SPS and RHIC energies has been performed in [14]. Here it turns out that at RHIC the results of the fit to the SM and the TSM are identical: the TSM simply splits the volume of the system in two equal parts with similar characteristics, which means that the particles are really emitted from one thermalized and homogeneous source. This gives us a temperature of $T = 176$ MeV and a baryo-chemical potential of $\mu_B = 39.8$ MeV [16]. The energy per hadron and the average hadron mass are $\langle E \rangle / \langle N \rangle = 1.12$ and $\langle M \rangle = 0.77$ GeV, respectively. As seen in Fig. 2, this is a significant rise compared to the values of $\langle E \rangle / \langle N \rangle$ and $\langle M \rangle$ obtained from the fit to experimental data on heavy-ion collisions at lower energies.

In contrast to RHIC, at lower energies results of the SM and the TSM do not coincide anymore, although both models seem to provide reasonable agreement with the data, as shown in Table I. Here it is worth noting that the TSM analysis has been performed for RHIC data taken in a very narrow midrapidity window. However, results of the TSM fitted separately to merely 4π -data

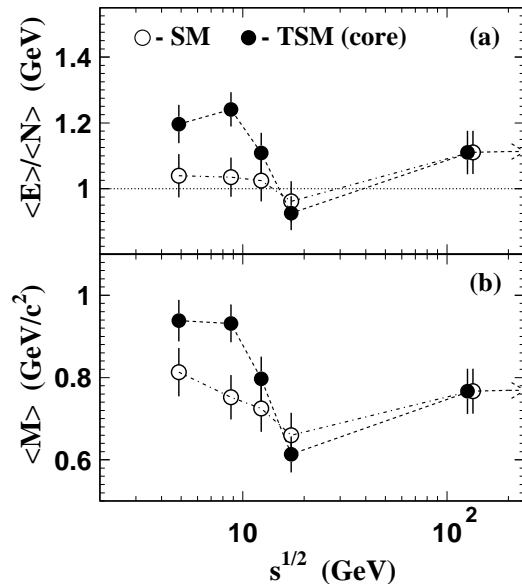


FIG. 2: (a) Average energy per hadron and (b) average hadron mass as functions of the center-of-mass energy of colliding nuclei. Full circles correspond to central source of the TSM, open circles denote the SM results. Lines are drawn to guide the eye.

and to midrapidity data, obtained in Pb+Pb collisions at SPS energies, indicate [14] that the temperature and the baryon chemical potential of the central source are varying insignificantly. Therefore, we do not expect considerable changes of the core conditions when the 4π -data at RHIC will be available. Macroscopic characteristics of the system obtained from the fit to the models are listed in Table II. For A+A collisions at $E_{lab} = 11.6$ AGeV, 40 AGeV, and 80 AGeV the energy per hadron and the average hadron mass in the central source (using the TSM) are about 20% larger than those obtained in the SM because of the following reasons: At such energies the TSM favours the formation of hot and dense core surrounded by a cooler halo. Moreover, the model indicates that the net baryon charge and the net strangeness are non-uniformly distributed within the system volume. Here three points should be mentioned: Using the TSM, all antibaryons are contained in the core, which is in accord with experimental data on, e.g., \bar{p} , \bar{d} , and $\bar{\Lambda}$ production [15, 23, 27]. The net strangeness in the core is small and negative. Such a scenario is confirmed by microscopic ultra-relativistic quantum molecular dynamics (UrQMD) [28] model predictions [29]. The negative strangeness in the central zone of a heavy-ion collision at energies below RHIC can be explained by different interaction cross sections of kaons and antikaons with baryons. In contrast, at RHIC energies and above the medium is meson dominated and the antibaryon yield at midrapidity is close to that of baryons. Hence, differences in the

TABLE I: Hadron yields and ratios for central heavy-ion collisions at 11.6A GeV, 40A GeV, and 80A GeV, respectively, and results of the fit to the two-source and the single-source statistical models of an ideal hadron gas.

	Data	TSM	SM	Ref.
Au+Au 11.6A GeV				
N_B	363 ± 10	364.1	362.9	[17]
p/π^+	1.234 ± 0.126	1.20	1.25	[18]
π^+	133.7 ± 9.9	131.6	123.3	[19]
K^+	23.7 ± 2.9	25.77	28.55	[17]
K^-	3.76 ± 0.47	3.725	3.824	[17]
Λ	20.34 ± 2.74	17.30	19.05	[20]
\bar{p}	0.0185 ± 0.002	0.0185	0.0183	[21]
Pb+Pb 40A GeV				
N_B	349 ± 5	351.6	352.8	[22]
$\bar{\Lambda}/\Lambda$	0.025 ± 0.0023	0.0258	0.0233	[23]
Λ/p (Pb+Au)	0.22 ± 0.05	0.212	0.232	[24]
π^-	312 ± 15	306.2	264.4	[22]
π^+	282 ± 15	276.2	239.0	[22]
K^+	56 ± 3	57.4	63.2	[22]
K^-	17.8 ± 0.9	18.2	19.4	[25]
$\bar{\Lambda}$	0.71 ± 0.07	0.727	0.71	[23]
Pb+Pb 80A GeV				
N_B	349 ± 5	351.6	352.8	[22]
π^-	445 ± 22	403.7	366.7	[26]
π^+	414 ± 22	375.6	341.1	[26]
K^+	79 ± 5	83.0	87.5	[26]
K^-	29 ± 2	33.4	35.4	[26]
Λ	47.4 ± 3.7	34.5	35.7	[23]
$\bar{\Lambda}$	2.26 ± 0.1	2.26	2.26	[23]

interaction cross sections are not important here leading to a homogeneous strangeness distribution over the whole reaction volume. Finally, the SM indicates that the net baryon density of the fireball formed in A+A collisions at 11.6A GeV and 40A GeV is about 10% below the normal nuclear density $\rho_0 = 0.17 \text{ fm}^{-3}$. At these energies hydrodynamic model calculations with and without the QGP formation [30] and microscopic model simulations [29, 31] favor, however, the formation of a much denser matter with central baryon densities of $\rho \approx 2\text{-}3 \rho_0$ at chemical freeze-out, which should take place around $t = 7\text{-}10 \text{ fm}/c$. Thus, the TSM predictions of a small central source with baryon densities of $\rho_B \cong 2.5 \rho_0$ quantitatively agree with these estimates. The volume of the central source varies from 300 fm^3 at AGS to 650 fm^3 at 40A GeV [32]. Therefore, to probe this zone one has to study hadron abundances and ratios in a quite narrow midrapidity window.

The baryon fraction in the hadrons yield is decreasing from 64.5% (59.3%) in the TSM (SM) at AGS to 13.7% at RHIC, while the antibaryon fraction rises from zero to 9.2%. Figure 3 depicts the hadronic densities at the chemical freeze-out stage in the central zone of heavy-ion collisions at $\sqrt{s} = 130A \text{ GeV}$ and at 40A GeV. The most abundant species are π , K , ρ , \bar{K} , η , and ω in the mesonic sector, and N , Δ , Σ , and Λ in the baryonic

Gorenstein, K. Redlich, D. Strottman, and N. Xu for the fruitful discussions. The work was supported by the Deutsche Forschungsgemeinschaft (DFG), Bundesministerium für Bildung und Forschung (BMBF) under the

contract No. 06TÜ986, and the National Science Foundation of China under the contracts No. 19975075 and No. 19775068.

-
- [1] Proceedings of the QM'99 conference (Torino, Italy, 1999) [Nucl. Phys. **A661**, 1c (1999)].
- [2] Proceedings of the QM'2001 conference (Stony Brook, NY, USA, 2001) [Nucl. Phys. **A698**, 1c (2002)].
- [3] J. Cleymans and K. Redlich, Phys. Rev. C **60**, 054908 (1999); Phys. Rev. Lett. **81**, 5284 (1998).
- [4] P. Braun-Munzinger, D. Magestro, K. Redlich, and J. Stachel, Phys. Lett. B **518**, 41 (2001).
- [5] P. Braun-Munzinger, I. Heppe, and J. Stachel, Phys. Lett. B **465**, 15 (1999).
- [6] L.D. Landau and S.Z. Belenkij, Usp. Phys. Nauk **56**, 309 (1955) [Nuovo Cim. Suppl. **3**, 15 (1956)].
- [7] J. Rafelski, Phys. Lett. B **62**, 333 (1991); J. Letessier and J. Rafelski, Phys. Rev. C **59**, 947 (1999).
- [8] F. Becattini, Z. Phys. C **69**, 485 (1996); F. Becattini and U. Heinz, Z. Phys. C **76**, 269 (1997); F. Becattini, M. Gazdzicki, and J. Sollfrank, Nucl. Phys. **A638**, 403 (1998).
- [9] J. Sollfrank, J. Phys. G **23**, 1903 (1997).
- [10] J. Cleymans, D. Elliot, H. Satz, and R.L. Thews, Z. Phys. C **74**, 319 (1997).
- [11] G.D. Yen and M.I. Gorenstein, Phys. Rev. C **59**, 2788 (1999).
- [12] S.R. de Groot, W.A. van Leeuwen, and Ch.G. van Weert, *Relativistic Kinetic Theory* (North Holland, Amsterdam, 1980).
- [13] L.V. Bravina *et al.*, Nucl. Phys. **A698**, 383c (2002); Phys. Rev. C **63**, 064902 (2001); J. Phys. G **27**, 421 (2001).
- [14] Z.-D. Lu, A. Faessler, C. Fuchs, and E.E. Zabrodin, nucl-th/0110040; Talk at Strangeness'2001 conference (Frankfurt a.M., Germany, 2001), [J. Phys. G. (in press)].
- [15] R. Arsenescu *et al.*, NA52 Collab., J. Phys. G **25**, 225 (1999).
- [16] Compared to [14], the multiplicity of negatively charged hadrons has been excluded from the present fit.
- With negatively charged hadrons the temperature and the baryon chemical potential rises to 185 MeV and 52.5 MeV, correspondingly.
- [17] L. Ahle *et al.*, E802 Collab., Phys. Rev. C **60**, 044904 (1999).
- [18] L. Ahle *et al.*, E802 Collab., Phys. Rev. C **60**, 064901 (1999).
- [19] L. Ahle *et al.*, E802 Collab., Phys. Rev. C **59**, 2173 (1999).
- [20] S. Ahmad *et al.*, Phys. Lett. B **382**, 35 (1996).
- [21] L. Ahle *et al.*, E802 Collab., Phys. Rev. Lett. **81**, 2650 (1998).
- [22] C. Blume *et al.*, NA49 Collab., Nucl. Phys. **A698**, 104c (2002).
- [23] A. Mischke *et al.*, NA49 Collab., nucl-ex/0201012.
- [24] K. Filimonov *et al.*, CERES/NA45 Collab., nucl-ex/0109017.
- [25] V. Friese *et al.*, NA49 Collab., Nucl. Phys. **A698**, 487c (2002).
- [26] T. Kollegger *et al.*, NA49 Collab., nucl-ex/0201019.
- [27] J. Bächler *et al.*, NA49 Collab., Nucl. Phys. **A661**, 45c (1999).
- [28] S.A. Bass *et al.*, Prog. Part. Nucl. Phys. **41**, 255 (1998); M. Bleicher *et al.*, J. Phys. G **25**, 1859 (1999).
- [29] L.V. Bravina *et al.*, Phys. Lett. B **434**, 379 (1998); J. Phys. G **25**, 351 (1999); Phys. Rev. C **60**, 024904 (1999).
- [30] L. Bravina, L.P. Csernai, P. Levai, and D. Strottman, Phys. Rev. C **50**, 2161 (1994).
- [31] L.V. Bravina, N.S. Amelin, L.P. Csernai, P. Levai, and D. Strottman, Nucl. Phys. **A566**, 461c (1994).
- [32] Note, that these numbers are obtained for an ideal gas of pointlike hadrons. If the Van der Waals type of the EOS with the non-zero hard core radius for hadrons is employed, the volume of the source increases.